

Experimental Evaluation of Induction Heating Systems with Phase-Shift Voltage Resonant Inverter

Alexandru BITOLEANU, Mihaela POPESCU, Vlad SURU *

* University of Craiova, Department for Electromechanical, Environmental and Industrial Informatics
Craiova, Romania, alex.bitoleanu@em.ucv.ro; mpopescu@em.ucv.ro; vsuru@em.ucv.ro

Abstract— This paper is devoted to the synthesis of the power control loop for a single-phase resonant inverter controlled by phase shift and used in an induction heating system. It starts from the assumption that, if the inverter control frequency is close to the resonance frequency of the assembly consisting of the compensation capacitor, inductor and heating piece, the current supplied by the inverter contains almost only the active component that determines directly the power transmitted to the inductor. After establishing the structural scheme and highlighting the transfer function, a PI controller is adopted for the control of the current through the inverter. The inverter active current is achieved by a Proportional-Integral controller tuned in accordance with the Modulus Optimum criterion in Kessler variant. Next, different experimental tests are presented in order to determine the performances of the induction heating system. The objectives of the tests were: the verification of the proper operation of the current through inverter control loop, the achievement of zero-current switching, the control of the power transmitted to the load by adjusting the inverter frequency and the determining the efficiency of the converter-inductor-pipe system.

I. INTRODUCTION

An experimental model for an induction heating system with single-phase voltage source inverter and parallel resonance was made through the research activity carried out within a project co-funded by European Regional Development Fund (Operational Programme Growth of the Economic Sector Competitiveness – POS CCE).

The voltage source inverters with resonant parallel load are used successfully in medium and high frequency induction heating systems [1]-[5]. The replacement of the current source inverters has been facilitated by both the existence on the market of the high power insulated-gate bipolar transistors (IGBTs) and the advantages of voltage source inverters [3], [5], [6]. They consist primarily in simple limiting the switching overvoltage and simplest achievement of switching at zero current. Last but not least, the use of parallel resonance allows for high load current with a small current through the inverter (only the active component). As the control system handles the operation of the induction coil in parallel with a compensation capacitor at the desired resonant frequency, the current through the induction coil is forced to be sinusoidal. In practice, the parallel resonant circuit is damped when the work piece is inserted into the induction coil by introducing additional losses into the system and increasing the

current drawn from the inverter [1], [3], [5], [7]. In order to obtain the auto-adaptation at the frequency required for zero current switching, the authors proposed an original method that has been successfully implemented. The paper is first focused on the tuning the control loop of the power transferred to a work pipe in the induction heating process through a voltage source resonant inverter. Next, a lot of experimental tests performed in order to confirm the performances of the system, are presented. For energetic and economic reasons, the inverter is supplied by an uncontrolled three bridge rectifier. Because the inverter operates at high frequency, especially in the superficially pipes heating, the phase-shift method was adopted for the inverter control. Starting from the block diagram based on transfer functions, the Modulus Optimum (MO) criterion is successfully applied in order to tune the PI current controller. The second section presents the experimental structure and gives some information about the experimental model and graphical interface used to implement the control algorithm on the real time dSPACE 1103 based system. Section 3 presents some experimental results and their processing and interpretation to determine the system performance. Finally some conclusions are drawn on future research directions.

II. BLOCK DIAGRAM AND CONTROL SYSTEM STRUCTURE

In the adopted structure of the induction heating system (Fig.1), a three-phase uncontrolled bridge rectifier supplies the IGBTs-based single-phase full-bridge voltage source inverter. In order to ensure zero-current switching, the operating frequency of the square-wave inverter, which is provided by an auto-adaptive loop, is imposed to be slightly higher than the resonant frequency of the equivalent circuit consisting of induction coil-work piece in parallel with the resonant capacitor. The control of the current through the induction coil can be performed by controlling its active component, which means the control of the inverter output current. As regards the required value of the induction coil current, there are two possible approaches. a) The work pipe moves through the inductor at a preset speed and the preset current depends on the required temperature gradient. b) The maximum rated current of the voltage inverter is preset and the work pipe speed is adjusted as a function of the required temperature gradient. This is the option that allows for maximum productivity in terms of the inverter.

The block diagram in Fig.2 illustrates the transfer functions of inverter current control loop [8], [9].

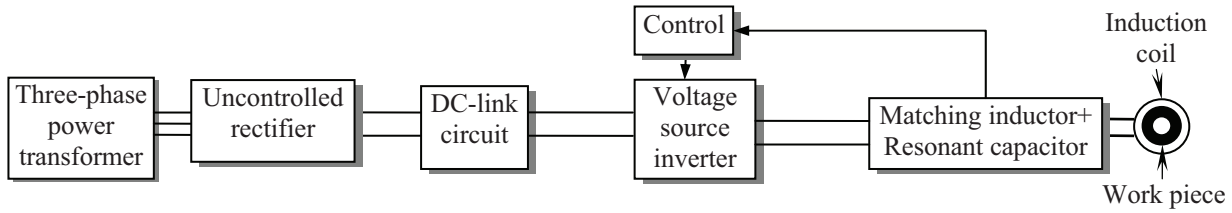


Fig. 1. Schematic diagram of the induction heating system..

A. Inverter Transfer Function

In order to obtain a controlled voltage at the inverter output, the phase-shift control technique was adopted [10], [11]. This technique is more appropriate compared to PWM, because the operation frequencies are high (about 5 kHz). The voltage shape at the output inverter associated to the phase-shift control contains one pulse on each half period, but the duration of each pulse may be less than or equal to π radians. (Fig. 2).

If U_i is the fundamental of inverter output voltage and supposing that the angle α is obtained by comparing the control voltage u_c (output of the current controller) with a

$$G_{MR}(s) = \frac{I_i(s)}{U_i(s)} = \frac{1/R_a \cdot (1 + T_{eb}s + T_{eb}T_{emb}s^2)}{R_b/R_a \cdot (1 + T_{emb}s) + (1 + T_{ema}s) \cdot (1 + T_{eb}s + T_{eb}T_{emb}s^2)}. \quad (2)$$

where $I_i(s)$ and $U_i(s)$ are the inverter output current and voltage in the Laplace domain.

The following specific constants are used: $T_{ema} = L_a/R_a$ - the electromagnetic time constant of the matching inductor; $T_{eb} = R_b \cdot C$ and $T_{emb} = L_b/R_b$ - the electric and electromagnetic time constants of the parallel resonant circuit. Note that L_b and R_b are associated to the equivalent inductance and resistance of the induction coil and heated piece and C is the capacitance of the resonant capacitor. The transducer was taken into consideration as first order element,

$$G_{Ti}(s) = \frac{K_{Ti}}{1 + sT_{Ti}}. \quad (3)$$

where, K_{Ti} and T_{Ti} are the proportional constant and time constant, respectively.

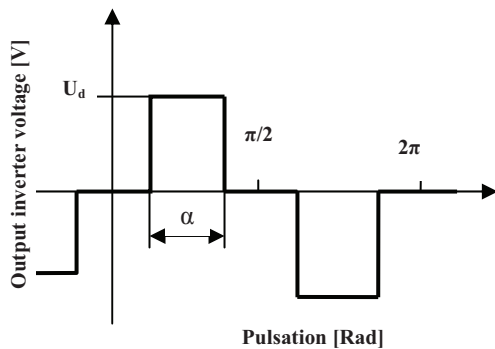


Fig. 2. The inverter voltage shape obtained by phase-shift control.

reference sinusoidal signal u_r , the transfer function of the inverter can be expressed as [8],

$$G_i(s) = \frac{2\sqrt{2}}{\pi} \frac{U_d}{U_{rM}} \frac{1}{1 + sT_\mu} = \frac{K_{inv}}{1 + sT_\mu}. \quad (1)$$

B. The Equivalent Matching and Resonant Circuit Transfer Function

The transfer function of the equivalent matching and resonant circuit ($G_{MR}(s)$) can be written in the following form [10]:

III. THE TUNING OF THE CURRENT CONTROLLER

As the transfer function of the open system has no pole in origin for cancellation the steady-state error, a Proportional-Integrative (PI) controller is adopted. In the same time, in order to remove the dominant time constants (the electromagnetic time constant of the matching inductor), the transfer function of the controller must be [8]:

$$G_{Ri}(s) = \frac{1 + k_{pi}T_i s}{sT_i}. \quad (4)$$

The current controller design is based on Modulus Optimum criterion in Kessler variant, which is dedicated to the rapid systems [13] and, finally, the values of the controller parameters are obtained as follows[8]:

$$T_i = 2 \cdot K_I \cdot T_\Sigma, \quad (5)$$

$$k_{pi} = \frac{T_{ema}}{2 \cdot K_I \cdot T_\Sigma}. \quad (6)$$

In this way, the current controller is completely determined.

IV. EXPERIMENTAL SETUP

The experimental model was built on the base of the electric scheme of the induction heating converter (Fig. 3).

This scheme highlights the following components:

1. Phase contactor K1, which makes the direct connection of the static converter (i.e. the resistances for charging the DC-link capacitor are decoupled by short circuit);

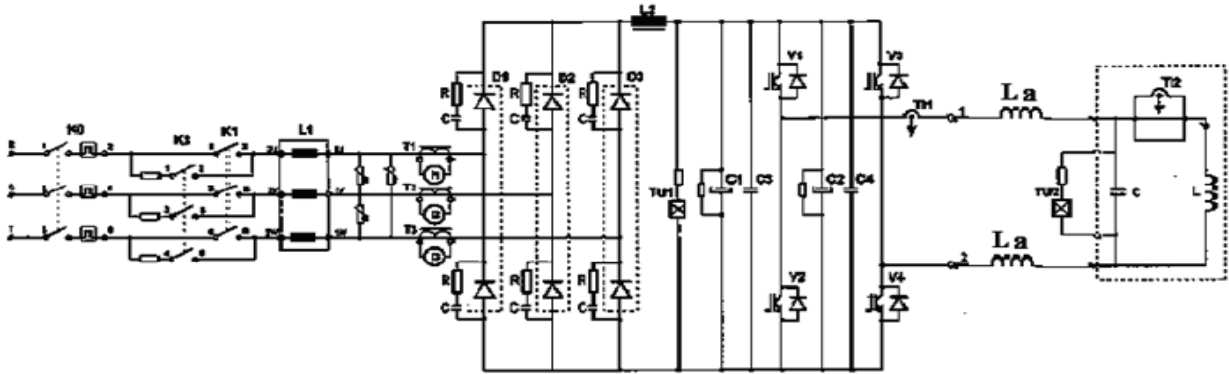


Fig. 3. The electric scheme of the induction heating converter for experimental setup.

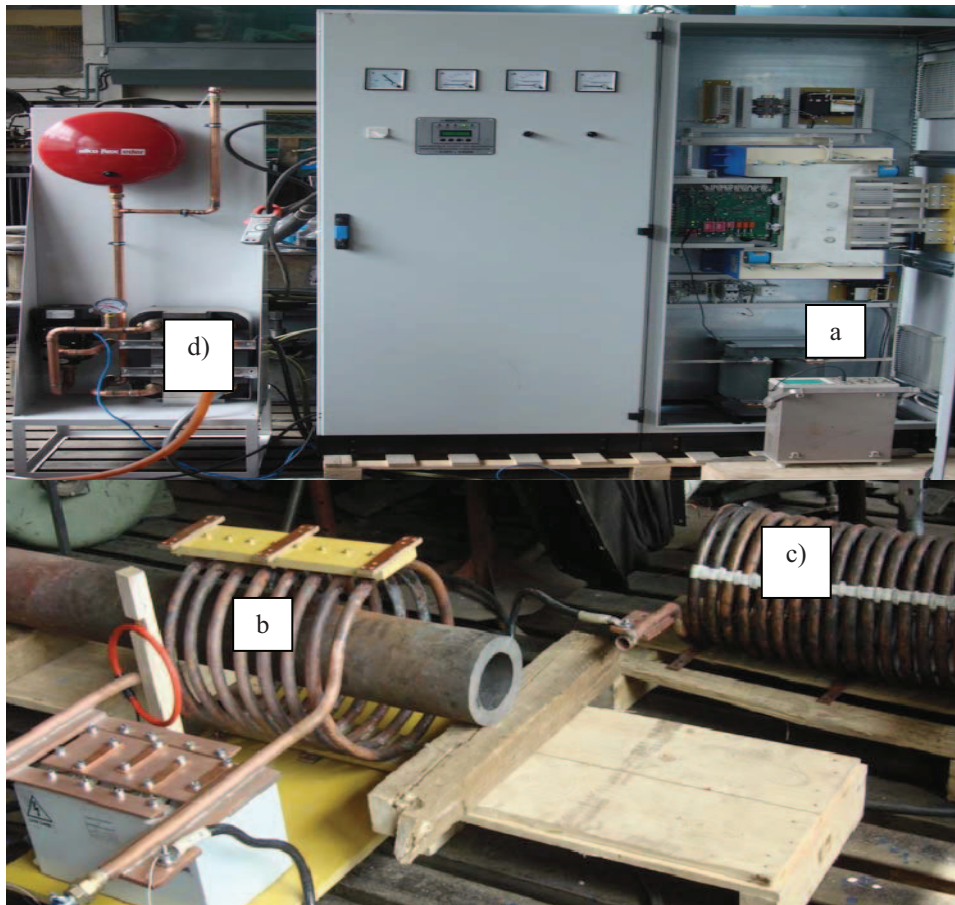


Fig. 4. Pictures of the experimental setup: a) inverter; b) inductor; c) matching coil; d) cooling equipment.

2. Phase contactor K3, which makes the intermediate circuit for DC-link capacitor charging;

3. Three-phase switching coil 0,08mH/350A (L1);

4. The static converter, which consists of a three-phase diode rectifier and the single-phase voltage source inverter with IGBTs (1200A, 1700V);

5. The DC-link circuit (L2, C1 and C2);

6. Compensation capacitors $C1=64\mu\text{F}$, $U=3000\text{V}$, $I=11,6\text{kA}$, $f=10\text{kHz}$ - 1 piece and $C2,3=31\mu\text{F}$; $U=1500\text{V}$; $I=2333\text{A}$; $f=8\text{kHz}$ - 2 pieces. By their combination, it may be useful to obtain three values of the equivalent capacity at 3000 V, i.e. $15.5\mu\text{F}$, $79.5\mu\text{F}$ and $64\mu\text{F}$;

7. The matching coil (L_a) which is provided with four intermediate sockets to check experimentally the existence of its optimal value [14];

8. The inductor, which is made from copper tube and it is cooled by water provided by an independent equipment (Fig. 4);

9. The required voltage and current transducers.

The control and management of the experimental model were carried out by a dSPACE 1103 system mounted in an industrial computer, in the laboratory of Power Electronics and Industrial Informatics of the Faculty of Electrical Engineering, University of Craiova [5], [6]. To interact with the experiment, a graphical user interface has been created.

V. EXPERIMENTAL RESULTS

The objectives of the tests were: verify the proper operation of the inverter current control loop, verify the achievement the zero current switching, verify the control of the power transmitted to the load by adjusting the inverter frequency and determine the efficiency of the converter-inductor-pipe system.

A. The verification of the proper operation of the current controller and zero current switching

In this test, the two control loops (frequency and current) operate simultaneously. The frequency control loop was put into operation by assigning a value greater than 1.1 for the ratio of forcing the capacitive component and the waveforms of the currents through inverter and inductor and the voltages across the inductor and inverter were recorded. Also, the time evolutions of the prescribed and actual inverter current and of the frequency were recorded.

The response of the current controller shows a good performance, both in rapidity and the absence of dangerous over current (Fig. 5, 6).

It is founded that, for the resulting frequency provided by the control loop (determined by load and coefficient of

forcing the capacitive active component), two situations may occur:

1. The inverter voltage is insufficient to achieve the prescribed current, even if the inverter transistors are closed during about 180° (Fig. 5, Fig. 7).

2. The inverter voltage is high enough, so that, in order to obtain the prescribed current, the inverter transistors are closed for less than 180° (Fig. 6).

For all these situations, it is shown that the frequency control loop and the current control loop operate properly.

The correlation between the operation frequency and the system performances is very important, especially in induction heating applications. Thus:

1. From the power factor point of view, the operation on resonant frequency is most advantageous because the inverter provides only the active current;

2. From the inverter losses point of view, the operation at a frequency slightly over the resonance value is most advantageous because the switching losses are minimized; it occurs if the zero current switching is achieved (Fig. 7); it is clear that the switch-on and the switch-off of the transistors occur at zero current;

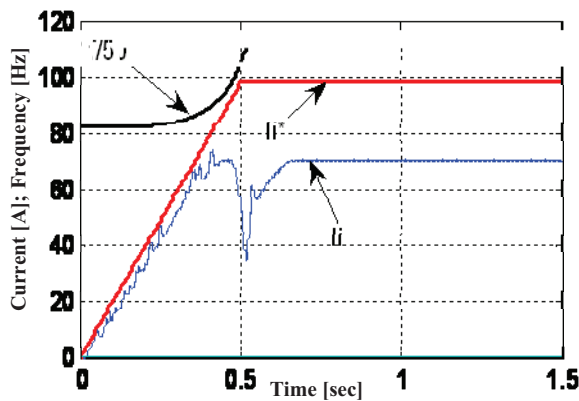


Fig. 5. The current and frequency response (experimental) when the voltage is insufficient.

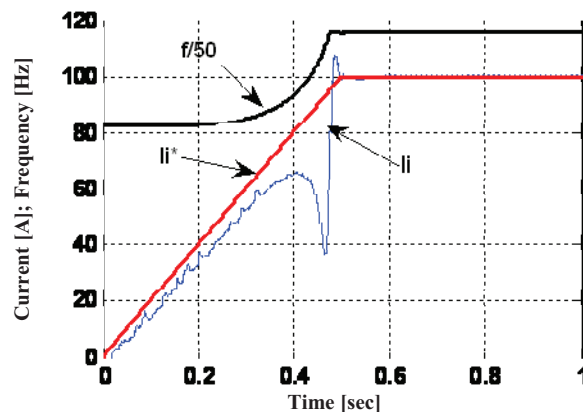


Fig. 6. The current and frequency response (experimental) when the inverter voltage is sufficient.

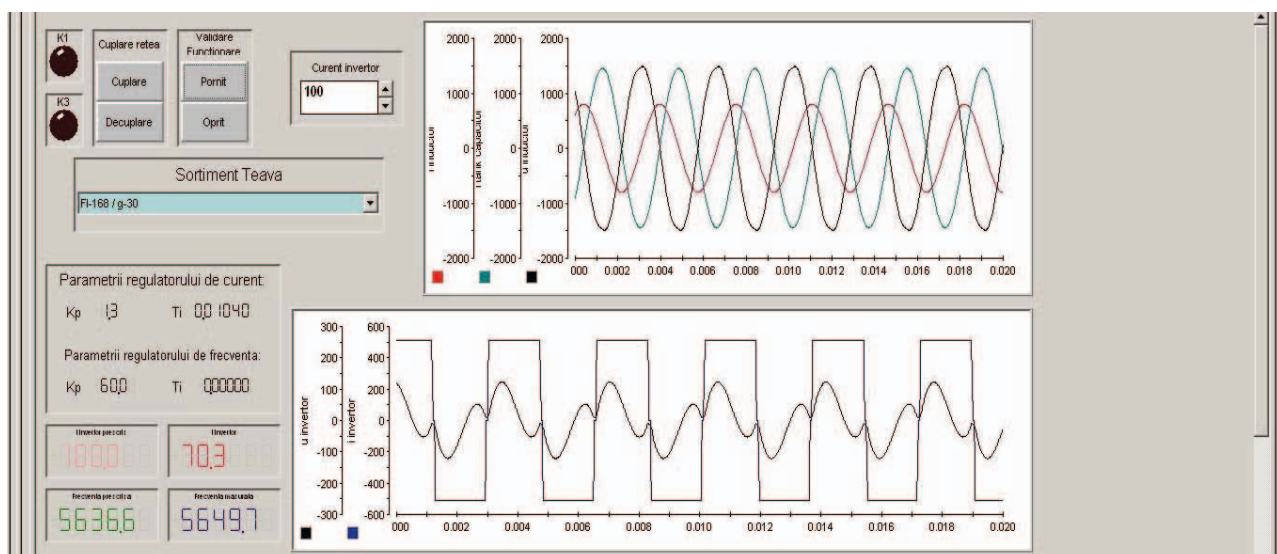


Fig. 7. The wave forms acquisitioned under control desk panel: the voltage across the inductor, the currents trough inductor and capacitor; the output inverter voltage and the current through it by highlighting that the inverter transistors are closed during about 180° .

B. The verification of the control of the power supplied to the load by adjusting the inverter frequency

In addition to the previous operation of the control circuit, the frequency is obtained by imposing, successively, three values of the coefficient of forcing the capacitive component (K_c). For each of the three cases, the following quantities were recorded: the currents through inverter and inductor, the voltages across the inductor and inverter. Then, the current through the capacitor and the RMS values of all quantities have been calculated, as well as the active power transmitted to the inductor (Table I).

The data in Table I confirm the possibility of controlling the active power transmitted to the load by adjusting the control frequency of the inverter over the resonance frequency of the inductor-pipe assembly. Thus, an increasing by about 3.6% of the frequency ($K_c = 1.4$ compared to $K_c = 1.2$), results in nearly doubling the power taken by the load.

Increasing the factor of forcing the capacitive behavior of the load has the following effects: increases the active power received by inductor; decreases depth of penetration; increases the transistors' switching current; increases the switching overvoltage; increases the losses in the inverter's transistors.

For example, when the coefficient of forcing the capacitive component increases from 1.2 to 1.4, the switching current increases about three times. Consequently, the power is adjustable by changing the inverter frequency control. However, although it is possible, there are some

drawbacks because of which this solution should be seen as a last option.

C. The determining the efficiency of the converter-inductor-pipe system

The test for determining the system efficiency was done by loading the inverter with a current of 300 A, by increasing the frequency up to about 6068 Hz. It must be specified that:

- The power quantities in the secondary of the transformer were measured with the analyzer Fluke 435 (Fig. 8);

- The following waveforms were recorded: the inductor and inverter currents, the inverter output voltage and the voltage across inductor;

- On the basis of the recorded waveforms, the active powers at the inverter output and the inductor input were calculated;

- Both the static converter efficiency and overall efficiency of the induction heating system were calculated (Table II);

- The current and the voltage at the inverter input were recorded (Fig. 9);

- The DC link current was acquired from a shunt and it contains some perturbations due to the transistors' switching (Fig. 9). To calculate the active power, it has been numerically filtered by means of a low pass filter with the cutoff frequency of 1.5 KHz.

TABLE I.
THE VALUES OF THE MAIN QUANTITIES FOR THREE VALUES OF THE FACTOR OF FORCING OF CAPACITIVE COMPONENT

K_c	f [Hz]	I_i [A]	I_b [A]	I_c [A]	U_b [V]	P_b [KW]
1,2	5732	80	649	772	450	10,5
1,3	5839	135,5	980	1255	562	15,6
1,4	5938	221	1270	1780	635	19,5

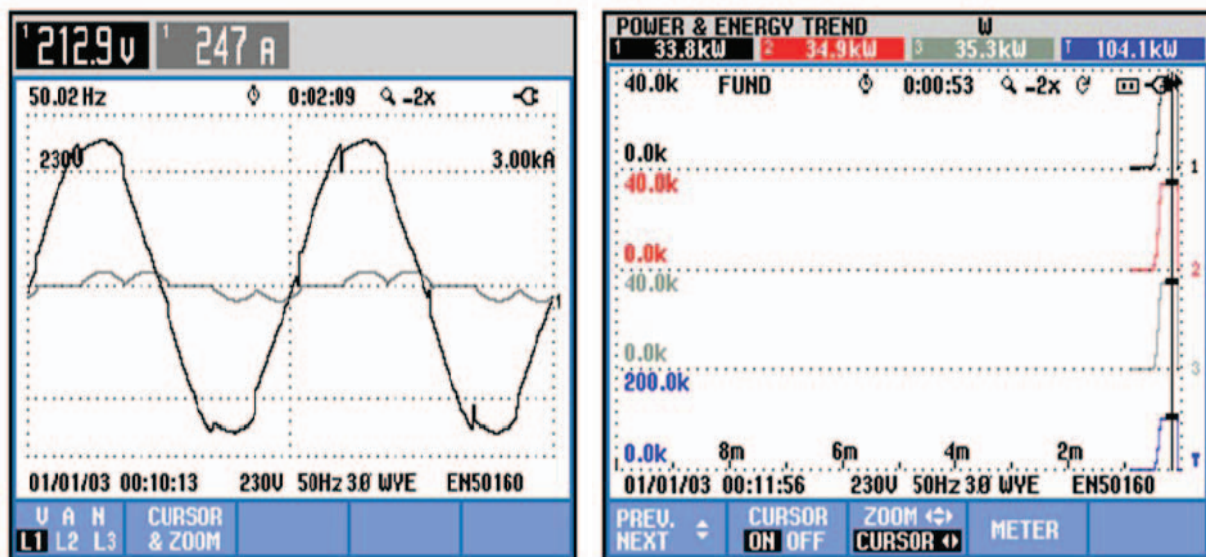


Fig. 8. Capture screen with the waveforms of current, voltage and the active powers in secondary of the transformer

TABLE II.
THE ACTIVE POWERS AND THE EFFICIENCIES

Quantity	Value
The active power in the secondary of transformer [KW]	104.1
The active power at output of the inverter [KW]	100.5
The active power taken of the inductor [KW]	78.5
The efficiency of the inverter [%]	96.5
The efficiency of the system [%]	75.4

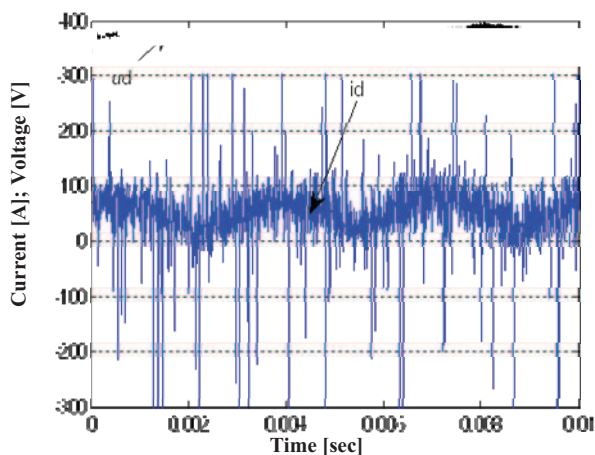


Fig. 9. The voltage and current in DC link circuit

VI. CONCLUSIONS

The experimental measurements performed on the induction heating system and the results obtained by their processing validate the adopted technical solution that includes original theoretical developments. The values of the efficiency, obtained for both inverter (96.5%) and entire system (75.4%), are very good [15]-[17]. These values show once again that the achieved system has superior energetic performance. With respect to the solution carried out as experimental model, two directions have been identified in order to improve it.

A. In the power part of the system

It is indisputable that, the solution proposed and achieved as an experimental model, respectively the use of a single-phase voltage source inverter with parallel resonance is most advantageous if the inverter operates at zero current switching.

Therefore, at high power supply, high voltages are required, so that the rated power is achieved at zero current switching and full wave inverter control (180° mode). For the analyzed profile of pipes, it is estimated that the DC link circuit voltage should be of about 1000V, respectively the line voltage in the transformer secondary of about 740 V.

B. In the control part of the system

Referring to the control algorithm of the system, a way to gain in flexibility is to identify a way of increasing the power automatically, even if the available voltage level is not enough for obtaining the desired current. It should be

possible if the control system would allow increasing the control frequency above the value which provides zero current switching. In principle, this method can be materialized by introducing a loop for calculating the coefficient of forcing the capacitive component of the current, based on the current error. It will be the subject of future investigations.

REFERENCES

- [1] J.M. Huerta, E.J.D. G. Santamaria, R. Garcia, J. C. Moreno, "Design of the L-LC Resonant Inverter for Induction Heating Based on Its Equivalent SRI," IEEE Trans. on Industrial Electronics[J], Vol. 54, No.6, 2007, pp.3178-3187.
- [2] J.M. Espi, E.J. Dede, E. Navarro, E. Sanchis, A. Ferreres, "Features and design of the voltage-fed L-LC resonant inverter for induction heating," Proc. Power Electronics Specialists Conference, 1999, pp.1126 - 1131.
- [3] S. Dieckerhoff, M.J. Ryan, R.W. De Doncker, "Design of an IGBT-based LCL-Resonant Inverter for High-Frequency Induction Heating," The 34th Industry Applications Conference, Vol. 3, Oct. 3-7, 1999, PP:2039-2045.
- [4] J.M. Espi, A.E. Navarro, J. Maicas, J. Ejea, S. Casans, "Control circuit design of the L-LC resonant inverter for induction heating," Proc. Power Electronics Specialists Conference, 2000, pp.1430-1435.
- [5] H. Yoo, E. Shim, J. Kang, G. Choi, C. Lee, B. Bang, "100kHz IGBT inverter use of LCL topology for high power induction heating," Proc. 8th IEEE International Conference Power Electronics and ECCE Asia, June 2011, pp. 1572-1575.
- [6] A. SALIH, "IGBT for high performance induction heating applications," Proc. 38th Annual Conference on IEEE Industrial Electronics Society, Oct. 2012, pp.:3274-3280.
- [7] V. Rudnev, D. Loveless, R. Cook, M. Black, Handbook of Induction Heating, Marcel Dekker, NY, 2003.
- [8] A. Bitoleanu, Mihaela Popescu, V. Suru, "Shift Phase Power Control in Induction Heating Systems with Voltage Resonant Inverter," Proc. of 2014 International Conference on Applied and Theoretical Electricity (ICATE), October 23-25, 2014
- [9] Mihaela Popescu, A. Bitoleanu, V. Suru, "Control of the Power in Induction Heating Systems with L-LC Resonant Voltage Source Inverters," 4th International Symposium on Electrical and Electronic Engineering, ISEEE 2013, Galati.
- [10] H. Kifune, Y. Hatanaka, "Optimal frequency tracking method for phase-shift PWM inverter," IEEJ Transactions on Electrical and Electronic Engineering, Volume 7, Issue S1, pages S167-S172, 21 December 2012.
- [11] H. Matsuo, H. Yonemori, Y. Yasaka, "Phase-shift controlled zero current switching high frequency inverter in the MHz frequency range," Power Electronics Conference (IPEC), 21-24 June 2010, pp. 2830-2835.
- [12] Mihaela Popescu, A. Bitoleanu, "Power Control System Design in Induction Heating with Resonant Voltage Inverter," Journal of Automation and Control Engineering Vol. 2, No. 2, June 2014, pp. 195-198.
- [13] A.J.J. Rezek, C.A.D. Coelho, J.M.E. Vicente, J.A. Cortez; P.R. Laurentino, "The modulus optimum (MO) method applied to voltage regulation systems: modeling, tuning and implementation," Proc. of Int. Conf. on Power System Transients, June 2001, pp.138-142.
- [14] A. Bitoleanu, Mihaela Popescu, V. Suru, "Maximizing Power Transfer in Induction Heating System with Voltage Source Inverter," Proc. of '22nd International Conference on Nonlinear Dynamics of Electronic Systems, Vol. 438, July 2014, pp. 134-141.
- [15] http://www.induction.it/OLD/melting_furnaces.htm
- [16] http://www.pillar.com/applications/documentlibrary/documentlibrary_docs/Pillar-MK-15.pdf
- [17] Callebaut J., Laborelec, Induction Heating, Power Quality & Utilization Guide, Section 7: Energy Efficiency, February 2007.